Can Gap Tuning Schemes of Long-range Corrected Hybrid Functionals Improve the Description of Hyperpolarizabilities?

Alejandro J. Garza,[†] Osman I. Osman,[‡] Abdullah M. Asiri,[‡,¶] and Gustavo E. Scuseria[*,†,‡,§]

Department of Chemistry, Rice University, Houston, Texas 77251-1892, USA, Chemistry Department, Faculty of Science, King Abdulaziz University, Jeddah 21589, Saudi Arabia, Center of Excellence for Advanced Materials Research (CEAMR), King Abdulaziz University, Jeddah 21589, Saudi Arabia, and Department of Physics and Astronomy, Rice University, Houston, Texas 77251-1892, USA

E-mail: guscus@rice.edu

Abstract

Long-range corrected hybrid density functionals (LC-DFT), with range separation parameters optimally tuned to obey Koopmans' theorem, are used to calculate the first-order hyperpolarizabilities of prototypical charge-transfer compounds p-nitroaniline (PNA) and dimethylamino nitrostilbene (DANS) in gas phase and various solvents. It is shown that LC-DFT methods with default range separation parameters tend to

[*]To whom correspondence should be addressed

[†]Department of Chemistry, Rice University, Houston, Texas 77251-1892, USA

[‡]Chemistry Department, Faculty of Science, King Abdulaziz University, Jeddah 21589, Saudi Arabia

[¶]Center of Excellence for Advanced Materials Research (CEAMR), King Abdulaziz University, Jeddah 21589, Saudi Arabia

[§]Department of Physics and Astronomy, Rice University, Houston, Texas 77251-1892, USA

underestimate hyperpolarizabilities (most notably in solution), and that the tuning scheme can sharply improve results, especially in the cases when the standard LC-DFT errors are largest. Nonetheless, we also identify pathological cases (two pyrrole derivatives) for which LC-DFT underestimates the hyperpolarizabilities, regardless of tuning. It is noted that such pathological cases do not follow the usual inverse relation between the hyperpolarizability and amount of exact exchange, and thus this behavior may serve as a diagnostic tool for the adequacy of LC-DFT.

Keywords

DFT, Optimal Tuning, Organic Materials, NLO, Charge Transfer, PCM.

Introduction

Because of their applications in nonlinear optics (NLO), conjugated charge-transfer organic compounds have generated much interest in industry and academia since the invention of lasers in the 1960s[1] and up to present day.[2–9] Specifically, this class of compounds are known to exhibit very large hyperpolarizability tensor β_{ijk} components (i.e., first-order NLO responses) along the direction of charge transfer,[10–14] and their applications include, e.g., frequency doubling of low power diode lasers, electrooptic modulation, optical signal processing, imaging enhancements, and frequency upconversion lasing.[15] But despite all the interest and research around NLO, the design of materials with tailor-made optical properties remains challenging. Furthermore, the accurate experimental determination of hyperpolarizabilities and other NLO characteristics can be difficult in some cases due to the many intricacies involved in the different techniques available for such determinations.[16] Hence, reliable theoretical predictions of NLO properties are particularly valuable in this field of research.

Obtaining accurate estimates for β_{ijk} by theoretical methods is, however, a challenge on its own. There are mainly two reasons for this: (1) hyperpolarizabilities are highly sensitive to electronic correlation effects[17] (even if purely dynamical), and (2) exact exchange plays an

important role in the description of charge-transfer excitations.[18–20] To complicate the issue further, organic charge-transfer compounds of interest in NLO are typically medium to large sized molecules, often ruling out the possibility of using high-level, computationally expensive, electronic structure methods to calculate their properties. Traditional density functional theory (DFT) methods, such as hybrids and generalized gradient approximations (GGAs), are applicable to large molecules and can account for (dynamic and some static) correlations. However, these methods have an incorrect asymptotic exchange potential behavior, which leads to an underestimation of charge-transfer excitation energies and, consequently, a large (at times catastrophic) overestimation of hyperpolarizabilities.[21–25] Although inclusion of 100% Hartree-Fock (HF) exchange should in principle fix this problem, in practice results are often unsatisfactory due to the reliance of DFT in the error cancellation between inexact exchange and correlation terms.

Long-range corrected (LC)-DFT methods[26–31] offer a possibility to restore the correct asymptotic exchange potential behavior and, simultaneously, avoid the inclusion of 100% Hartree-Fock exchange. In LC-DFT, the interelectronic Coulomb operator r_{12}^{-1} is partitioned into a short-range (SR) component and its long-range (LR) complement

$$\frac{1}{r_{12}} = \underbrace{\frac{1-\mathrm{erf}(\omega r_{12})}{r_{12}}}_{SR} + \underbrace{\frac{\mathrm{erf}(\omega r_{12})}{r_{12}}}_{LR}, \tag{1}$$

where erf is the error function and ω a parameter defining the range separation (not to be confused with the symbol often used to denote the frequencies in frequency-dependent hyperpolarizabilities). In spite of being a trivial equality, Eq. 1 allows for meaningful manipulations of a functional since one can now evaluate the exchange energy as

$$E_x^{\mathrm{LC-DFT}} = E_x^{\mathrm{SR-DFT}}(\omega) + E_x^{\mathrm{LR-HF}}(\omega). \tag{2}$$

Thus, the amount of exact exchange included in $E_x^{\mathrm{LC-DFT}}$ increases with the interelectronic

distance, leading to the correct asymptotic behavior for the exchange potential and an improved description of charge-transfer processes. Numerous studies have found that LC-DFT methods provide better estimates for hyperpolarizabilities and related properties in charge-transfer compounds as compared to hybrid and GGA functionals.[18,32–42] However, some recent works have also concluded that LC-DFT does not consistently outperform hybrids and GGAs; for example, in Ref. 43, the range-separated CAM-B3LYP provides the best results in some solvents, but the standard hybrid B3LYP is better in others. These two seemingly contradictory observations may be reconciled by considering the fact that the optimal range separation parameter ω in LC-DFT has been shown to be strongly system dependent.[44] Therefore, if the optimal ω value for a certain system is close to zero and far from the default value obtained via the functional's original parametrization, one could expect a GGA functional to be more adequate than its LC-GGA counterpart. This, of course, poses the question of how to determine the optimal range separation parameter.

A nonempirical methodology to estimate the optimal ω for a determined system has been proposed by Stein et al.[45–48] (for a recent review, see Ref. 49). The scheme relies on demanding that the molecule, and its corresponding anion, obey Koopmans' theorem.[50] The difference between the HOMO and LUMO energies in optimally tuned LC-DFT by the aforementioned criterion provides a good approximation to the fundamental gap (the difference between ionization potential and electron affinity). Thus, these methods are sometimes referred to as "gap tuning" schemes. It has been shown that these techniques greatly improve the accuracy of transition energies in charge-transfer excitations.[45–48,51–53] Furthermore, a recent study by Sun and Autschbach[54] indicated that gap tuning methods can also yield better hyperpolarizabilities than LC-DFT with default parameters for prototypical charge-transfer compounds such as p-nitroaniline (PNA) and dimethylamino nitrostilbene (DANS). We note, however, that Nénon et al.[55] found tuned LC-DFT to be inadequate for the calculation of polarizabilities (α_{ij}) and second-order hyperpolarizabilities (γ_{ijkl}) in large π-conjugated chains.

In the present paper, we explore further the possibility of improving the description of

hyperpolarizabilities, specifically first-order hyperpolarizabilities, by tuned LC-DFT. The main contributions of this work are the following: (1) some of the above mentioned results by Sun and Autschbach[54] are confirmed, (2) it is shown that the improvement of tuned over standard LC-DFT for describing β_{ijk} in charge-transfer compounds is much more dramatic in polar media (solvent effects were not investigated in Ref. 54), and (3) a cautionary note on pathological cases for LC-DFT (tuned or not) is provided, along with a possible diagnostic tool to identify such cases. The specific effects of solvent and wavelength, which have been shown to significantly affect the quality of DFT predictions,[43] on frequency dependent hyperpolarizabilities are also investigated. For these purposes, we study PNA and DANS in various media as model systems for charge-transfer compounds. Two recently synthesized[56,57] charge-transfer pyrrole derivatives, **1** and **2** (see Figure 1), comprise the pathological cases that appear to be difficult to handle for LC-DFT. These will serve to illustrate the application of our proposed diagnostic tool.

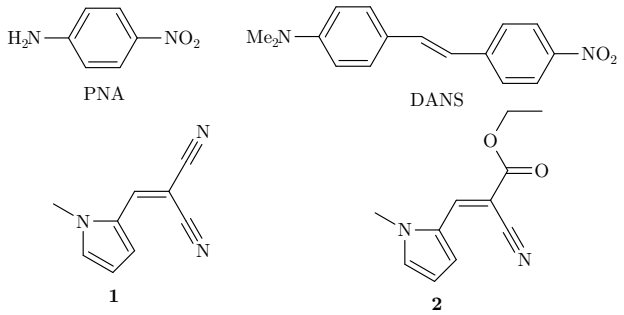

Figure 1: Molecular structures of the compounds studied in this work.

Theory and Methods

Hyperpolarizabilities

The use of different conventions for reporting hyperpolarizabilities has been recognized as the source of much confusion, leading to erroneous experiment-theory and experiment-experiment comparisons.[58–60] To avoid these issues, we dedicate this section to clarify the

conventions and hyperpolarizability measures employed here.

All hyperpolarizabilities in this work are reported in the "T" convention. The name for this convention comes from the fact that it defines (hyper)polarizabilities based on the Taylor expansion of the induced dipole moment $\boldsymbol{\mu}$ as a function of the field $\boldsymbol{F}$

$$\mu_i(\boldsymbol{F}) = \mu_i^0 + \alpha_{ij}F_j + \frac{1}{2!}\beta_{ijk}F_jF_k + \frac{1}{3!}\gamma_{ijkl}F_jF_kF_l + \cdots \tag{3}$$

where $\boldsymbol{\mu}^0$ is the dipole moment in the absence of the field, $\boldsymbol{\alpha}$ the polarizability, $\boldsymbol{\beta}$ the first-order hyperpolarizability, $\boldsymbol{\gamma}$ the second-order hyperpolarizability, and so on. The T convention is most prevalent in computational quantum chemistry, although one should be aware that a phenomenological convention (called like that because it absorbs numerical factors in the hyperpolarizability definitions), the X convention, is also commonly used by experimentalists. For second harmonic generation first-order hyperpolarizabilities, the T and X conventions are related by $\beta^T(-2w;w,w) = 4\beta^X(-2w;w,w)$; further details about the relations between conventions may be found in the paper by Reis.[60]

Regarding the actual hyperpolarizability measures used here, consider the component of the first hyperpolarizability along the permanent dipole moment in the T convention

$$\beta_z^T = \beta_{zzz} + \frac{1}{3}\left(\beta_{zxx} + 2\beta_{xzx} + \beta_{zyy} + 2\beta_{yzy}\right). \tag{4}$$

We report the often used quantity denoted as $\beta_{||}$, which is given in terms of β_z^T as $\beta_{||} = (3/5)\beta_z^T$. Additionally, in some calculations, we also provide the total hyperpolarizability β_{tot} given as

$$\beta_{tot} = \sqrt{\beta_x^2 + \beta_y^2 + \beta_z^2} \tag{5}$$

where

$$\beta_i = \beta_{iii} + \frac{1}{3}\sum_{i\neq j}(\beta_{ijj} + \beta_{jij} + \beta_{jji}). \tag{6}$$

The β_{tot} values given here are frequency independent and the coordinate system is defined

by the standard orientation of the molecules. This is purely a convenience based on the way hyperpolarizability tensors are printed in the output file generated by the program used for the calculations (see Computational details section). For $\beta_{||}$, some of the reported values are static while other are frequency dependent; this is explicitly stated in every relevant case to avoid any kind of ambiguity. As is customary in quantum chemistry, hyperpolarizabilities are given in atomic units (a.u.), which are related to the electrostatic units (esu) through the relations 1 a.u. $= 1.4818 \times 10^{-25}$ esu for α, 1 a.u. $= 8.6393 \times 10^{-33}$ esu for β, and 1 a.u. $= 5.0367 \times 10^{-40}$ esu for γ.

Gap tuning schemes

As stated in the Introduction, the gap tuning schemes of LC-DFT demand that the molecule, and its corresponding anion, obey Koopmans' theorem.[45–48] The physical motivation behind these criteria lays on the fact that this theorem holds for exact Kohn-Sham DFT.[61,62] Recall that Koopman's theorem states that the energy of the HOMO is equal in magnitude and opposite in sign to the ionization potential (this leads to the first criterion, that is, that the molecule obey Koopman's theorem). A more accurate IP can be thought of as improving the description of the donor group in a charge-transfer compound. Likewise, precise electron affinities (EAs) could be related to a better description of the properties of the acceptor. Since no analogous rule to Koopman's theorem exists for EAs, one requires instead the anion of the system of interest to obey the aforementioned theorem (the second criterion). The range-separation parameter ω provides the free variable to optimize in order to satisfy these constrains. Thus, mathematically, ω is chosen as the minimizer of the function

$$J_{gap}(\omega) = J_{IP}(\omega) + J_{EA}(\omega) \tag{7}$$

with

$$J_{IP}(\omega) = \left|\epsilon_H^{\omega}(N) + E_{\omega}(N-1) - E_{\omega}(N)\right|, \tag{8}$$

$$J_{EA}(\omega) = |\epsilon_H^\omega(N+1) + E_\omega(N) - E_\omega(N+1)| \tag{9}$$

where ϵ_H^ω is the energy of the HOMO and $E_\omega(N)$ the total energy for the N-electron system. Note that this procedure for determining ω makes no reference to empirical data, thus providing a physically sound ω without the bias introduced by traditional parametrizations based on selected benchmark sets.

A simple argument to motivate the use of gap tuning for improving the description of hyperpolarizabilities can be derived using the two-level model.[10,58,60] This model, also known as the two-state approximation, is based on a sum-over-states expression assuming that the hyperpolarizability can be well approximated by considering only one excitation (the main charge-transfer excitation). In the static frequency limit, the two-level model approximates β_z^T as[60]

$$\beta_z^T = \frac{6\mu_{eg,z}^2(\mu_{e,z} - \mu_{g,z})}{w_{eg}^2}, \tag{10}$$

where $\mu_{eg,z} = \langle\Psi_e|\hat{\mu_z}|\Psi_g\rangle$, $\mu_{e,z}$ and $\mu_{g,z}$ are transition and dipole moments for the excited and ground states in the z direction, and w_{eg} is the transition energy $|\Psi_g\rangle \rightarrow |\Psi_e\rangle$. Although Eq. 10 does not yield quantitative results (it largely overestimates β_z^T), it usually reproduces qualitative trends correctly and accounts for a large part of the hyperpolarizability in a converged sum-over-states expression.[52,63,64] In any case, the hyperpolarizability in Eq. 10 depends on the inverse of the square of the transition energy w_{eg}, which is known to be improved by gap tuning schemes.[45–48,51–53] Thus, one could expect more accurate hyperpolarizability predictions from tuned LC-DFT functionals as compared to their unoptimized counterparts.

Computational details

All calculations were carried out using the Gaussian 09 suite of programs.[65] Two GGAs, one traditional hybrid, and three LC-DFT functionals are used in this work; these are, respectively, PBE, B97-D, B3LYP, CAM-B3LYP, ωB97X-D, and LC-ωPBE. The Gaussian code

was modified in order to compute hyperpolarizabilities using the LC-ωPBE functional, and also to calculate the charge-transfer indices of Le Bahers et al.[66] Unless otherwise noted, the geometries utilized in the calculations were optimized at the CAM-B3LYP/6-31G(d,p) level of theory using standard thresholds defined by Gaussian's `Opt` keyword. Hyperpolarizabilities were also evaluated at the MP2 level of theory, to use as reference in certain of the benchmark calculations. Default parameters given by the `Polar` keyword are used in the computation of hyperpolarizabilities; this implies the analytical evaluation of these quantities for DFT methods, but numerical for MP2. These calculations employ the 6-311+G(d,p) and 6-311++G(d,p) basis sets, which have been shown to be adequate for the prediction of first-order NLO properties.[67] Calculations on the excited states of **1** and **2** were performed using time dependent density functional theory (TDDFT). The densities of the ground and excited states were analyzed using Gaussview[68] to visually characterize the charge transfer nature of the excitations. All computations reported to be done in solvent media utilized the polarizable continuum model (PCM; `SCRF` keyword) to mimic solvation effects.[69] We note that the PCM results shown here correspond to the non-equilibrium solvation limit, which is the default option for TDDFT in Gaussian when excited state geometries are not optimized.

Regarding the optimization of the range separation parameter, we take here a minimalist approach and select the ω value that minimizes J_{gap} among the set $\omega/\text{bohr}^{-1} = \{1 \times 10^{-4}$, 0.1, 0.2, 0.3, 0.4, 0.5$\}$; the internal options (IOps) of the Gaussian software are used to set the ω values (1×10^{-4} is the smallest value that can be requested). We use this approach for the following reasons: (1) predicted properties do not change radically for ω values that differ by about ± 0.01 bohr^{-1}, (2) this same methodology has been shown to be appropriate for describing other charge-transfer compounds,[52] (3) it is computationally inexpensive, and (4) we compare mostly against experimental hyperpolarizabilities, which have certain margin of error, making a finer tuning of ω not meaningful. From now on, we shall use an asterisk (*) to distinguish between tuned and non-tuned LC-DFT methods. Hence, for example, LC-ωPBE* and ωB97X-D* utilize range separation parameters that minimize J_{gap}, rather

than their default 0.4 and 0.2 bohr^{-1} ω values, respectively.

Results and discussion

PNA in gas phase and solution

In this section, we assess the performance of LC-ωPBE* and ωB97X-D* against traditional GGAs, hybrids, and non-tuned LC-DFT functionals in the prediction of the first-order hyperpolarizabilities of PNA. For convenience, the optimal ω values utilized are listed in Table 1; in general, the range separation parameter is smaller in more polar media (although this may be partly an effect of the insufficiency of PCM to describe the solvent; *vide infra*). Table 2 compares the experimental[43,59,60,70–73] $\beta_{||}$ values for PNA in various solvents and at different wavelengths with data predicted by DFT functionals. Globally, tuned LC-DFT methods (LC-ωPBE* and ωB97X-D*) provide the best agreement with experiment, having mean absolute errors (MAEs) of about 15%. This represents a substantial improvement over non-tuned LC-DFT (MAEs of 27 and 21% for LC-ωPBE and ωB97X-D, respectively), which tend to underestimate hyperpolarizabilities in solution; the mean error (ME = theory − experiment) for LC-ωPBE is −27%. On the other hand, pure GGAs have an opposite tendency and overestimate $\beta_{||}$ (ME = 23%, MAE = 29% for PBE; ME = 24%, MAE = 30% for B97-D). It seems therefore that tuned LC-DFT can alleviate some of the problems of standard LC-DFT and GGAs. We also note that the traditional hybrid B3LYP provides rather good agreement with experiment in solution, but poor results for the gas phase. Furthermore, B3LYP is ultimately outclassed by the tuned LC-DFT methods.

Table 1: Optimal range separation parameters (bohr^{-1}) for PNA.

Media	LC-ωPBE	ωB97X-D
Gas	0.3	0.2
1,4-Dioxane	0.1	0.1
Acetone	0.1	1×10^{-4}
Methanol	1×10^{-4}	1×10^{-4}

Table 2: Comparison of experimental and theoretical $\beta_{||}$ data (in a.u.) for PNA in different media and at various wavelengths (nm). All calculations use the 6-311+G(d,p) basis. The original experimental values are from various references,[59,70–73] but have been conveniently compiled and corrected/adapted from different conventions in Refs. 43,60.

Media	λ	Expt.	PBE	LC-ωPBE	LC-ωPBE*	B97-D	ωB97X-D	ωB97X-D*	B3LYP
Gas	1,064	1,072	2,131	1,090	1,222	2,140	1,262	1,262	1,744
1,4-Dioxane	Inf.	2,250	1,912	1,343	1,844	1,922	1,504	1,690	1,840
1,4-Dioxane	1,064	2,760	4,314	2,032	3,834	4,332	2,422	2,943	3,472
1,4-Dioxane	1,907	1,596	2,270	1,471	2,165	2,280	1,668	1,902	2,112
Acetone	Inf.	3,305	3,804	2,606	3,723	3,828	2,990	3,517	3,718
Acetone	1,064	4,317	4,836	2,461	4,438	4,851	2,935	3,746	4,109
Acetone	1,907	2,162	2,423	1,742	2,390	2,430	1,960	2,260	2,392
Methanol	Inf.	4,027	3,952	2,704	3,980	3,980	3,107	3,656	3,870
Methanol	1,064	5,334	4,717	2,434	4,772	4,731	2,897	3,680	4,035
ME (a.u.)	- -	- -	393	-993	172	408	-675	-241	52
MAE (a.u.)	- -	- -	622	997	397	625	734	461	513
ME (%)	- -	- -	23	-27	9	24	-16	-3	10
MAE (%)	- -	- -	29	27	16	30	21	15	22

Given that tuned LC-DFT has the best overall performance in the calculations presented in Table 2, it is interesting to investigate further the correlation between J_{gap} and the error in hyperpolarizabilities, and its dependence on solvent and frequency. Figure 2 shows the relationship between J_{gap} and the error in DFT hyperpolarizabilities ($\beta_{||}$) with respect to experiment (error = theory − experiment) for PNA. All three panels in this figure show the same data, but classified differently by functional, media, and wavelength, in order to facilitate the inspection of the data and reveal important trends. These trends (which will in short be analyzed in detail) are the following:

- LC-DFT functionals tend to underestimate (i.e., yield negative errors) $\beta_{||}$ in solution when J_{gap} is large. This error becomes more positive (increasing roughly linearly) as J_{gap} decreases, providing overall better results. Hybrids and GGAs also display larger absolute errors when J_{gap} is large. In fact, data with errors that are within 20% of the experimental $\beta_{||}$ are clustered around the region $J_{\text{gap}} \leq 0.05$ Hartree.

- At a given wavelength, the error in $\beta_{||}$ in methanol is more negative as compared to the less polar acetone.

- For LC-DFT data in a given solvent, the error in $\beta_{||}$ is more negative at 1,064 nm than at 1,907 nm or infinite wavelength.

It is worth noting that, although hybrids and GGAs are generally considered inadequate for calculating hyperpolarizabilities, results from these functionals are seen to be quite reasonable when J_{gap} is not very large. This occurs only in solution so that it may be possible that the strong charge-transfer predicted by hybrids and GGAs is unphysical in the gas phase, but is made possible in solution by means of the stabilization provided by polarization of the solvent by the solute. However, LC-DFT has the advantage that it can be tuned to reduce J_{gap} in different media, something that cannot be done with standard hybrids and GGAs.

A more detailed quantification of the dependence of the quality of DFT $\beta_{||}$ predictions on frequency and solvent is carried out in Figure 3. In this figure, the MEs and MAEs for the hyperpolarizability data at 1,064 nm and infinite wavelength in 1,4-dioxane, acetone and methanol are plotted to analyze the interactions between these variables and different functionals. It is seen from the top right panel of Figure 3 that GGAs and non-tuned LC-DFT functionals have opposite trends in the mean error as function of wavelength; for LC-DFT the error is more negative at 1,064 nm than at infinite wavelength. This observation indicates that GGAs exaggerate the increase in hyperpolarizability when going from the static limit to 1,064 nm, whereas LC-DFT underestimates this effect. Tuned LC-DFT and hybrids ameliorate these issues, providing overall lower absolute errors. From the top right panel of Figure 3, it can also be appreciated that all functionals provide lower MAEs at infinite wavelength (i.e., in the static limit).

The relationship between solvent and DFT error, analyzed in the two panels at the bottom of Figure 3, is also an interesting one. All functionals display significantly more negative MEs ($\sim$ 10-20%) in methanol ($\varepsilon = 35.69$) than in acetone ($\varepsilon = 20.49$) or 1,4-dioxane ($\varepsilon = 2.21$). In fact, all functionals tend to underestimate hyperpolarizabilities in the highly polar methanol. However, GGAs and tuned LC-DFT with very low amounts of HF exchange (PBE, B97-D, and LC-ωPBE*) do provide good results in this solvent. Note also

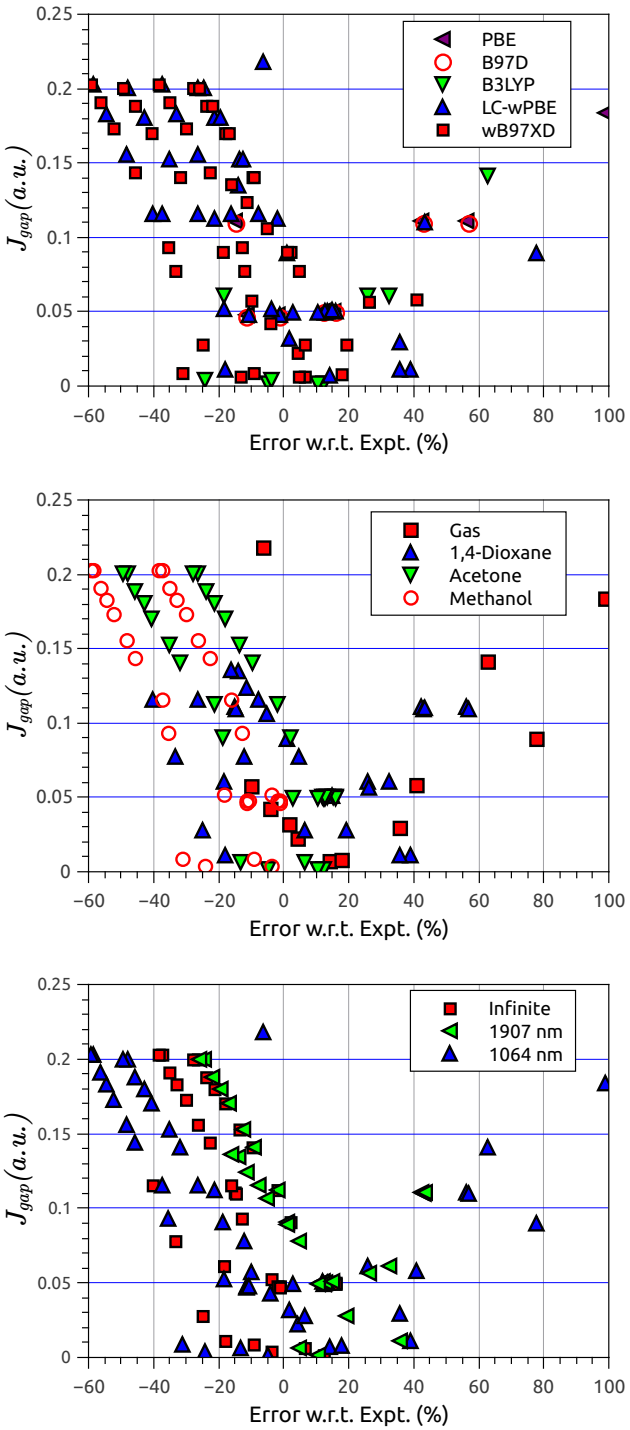

Figure 2: Relationship between J_{gap} and the error (theory − experiment) in $\beta_{||}$ values calculated by DFT for PNA. All three panels show the same data, but classified differently by functional, media, and wavelength.

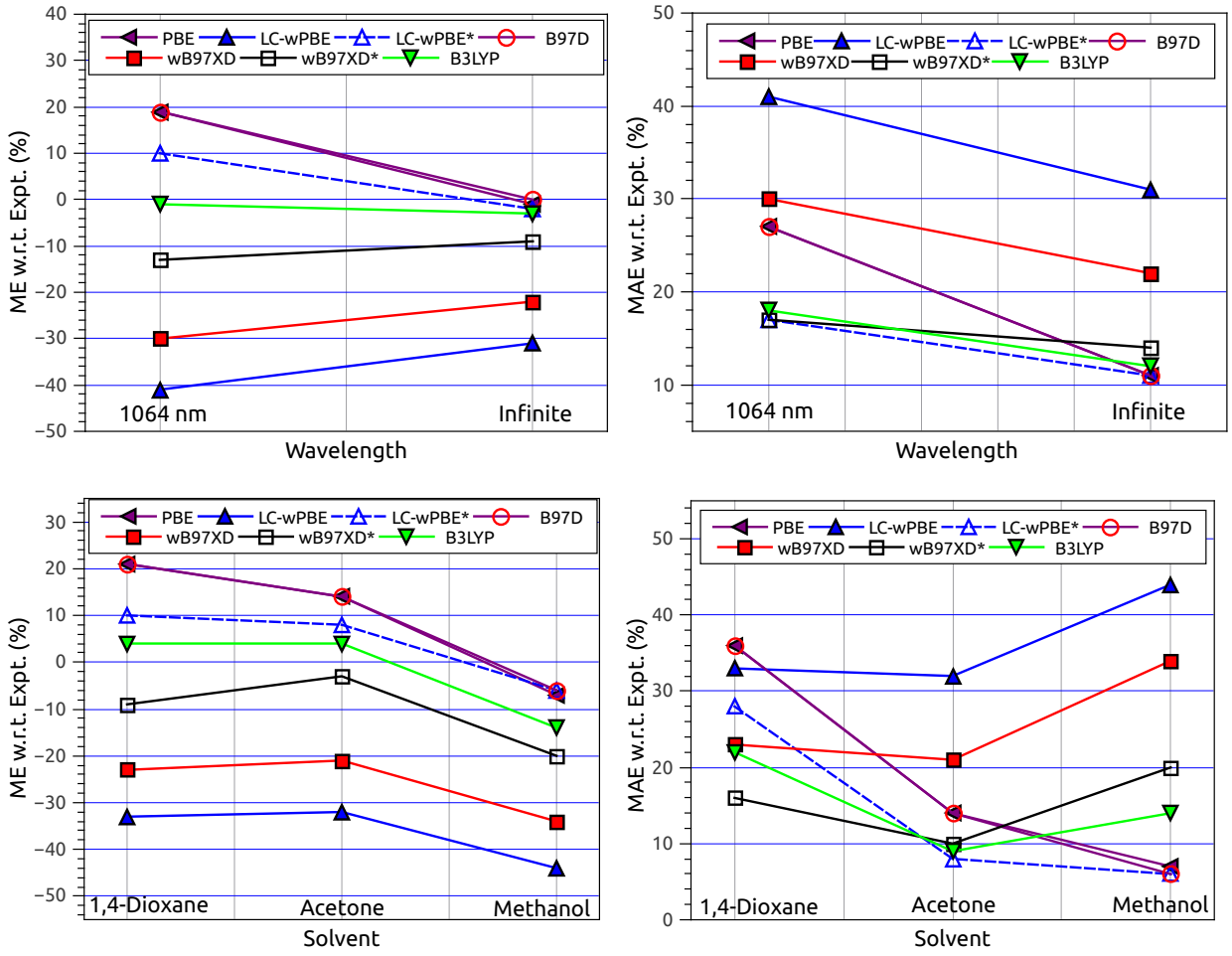

Figure 3: Average errors for the DFT $\beta_{||}$ data of PNA at 1,064 nm and infinite wavelength in 1,4-dioxane, acetone, and methanol. ME is the mean error (theory − experiment) and MAE the mean absolute error.

the very large improvements of tuned LC-ωPBE over its non-tuned version, which become more noticeable as the dielectric constant of the media increases; the MAEs are reduced by 5, 24, and 38% in 1,4-dioxane, acetone, and methanol, respectively. The same can be said about ωB97X-D and its tuned variant ωB97X-D*, except that the improvements are more moderate in this case because the default $\omega = 0.2$ a.u. in ωB97X-D is closer to its optimal values in solution than that of LC-ωPBE (0.4 a.u.). Also, ωB97X-D* underestimates $\beta_{||}$ in methanol more strongly than LC-ωPBE*, most likely due to the inclusion of a higher amount of HF exchange in the former via its short-range part, which is hybrid.

Table 3: Differences in averages of errors (ME/MAE in percentage with respect to experiment) in $\beta_{||}$ at 1,064 nm and infinite wavelength, and in different media for PNA calculated using data from Table 2. All calculations use the 6-311+G(d,p) basis and CAM-B3LYP/6-31G(d,p) geometries.

Difference	PBE	LC-ωPBE	LC-ωPBE*	B97-D	ωB97X-D	ωB97X-D*	B3LYP	Mean
1,064 nm − Inf.[†]	20/16	-10/10	13/7	19/16	-8/8	-3/3	2/7	4.6/9.6
Dioxane − Gas[‡]	-42/42	-28/25	25/25	-43/43	-30/-5	-11/-11	-37/-37	-23.8/-12.7
Acetone − Gas[‡]	-87/-87	-45/41	-11/-11	-87/-87	-50/14	-31/-4	-68/-58	-54.0/-27.4
MeOH − Gas[‡]	-110/-87	-56/53	-25/-3	-111/-88	-63/28	-49/13	-87/-28	-71.6/-17.6
Acetone − Dioxane[§]	-7/-22	1/-1	-3/-21	-7/-22	2/-2	6/-6	0/-13	-1.1/-12.4
MeOH − Acetone[§]	-20/-7	-12/12	-14/2	-20/-8	-13/13	-17/10	-18/5	-16.3/3.5
MeOH − Dioxane[§]	-27/-29	-10/10	-16/-23	-27/-30	-12/12	-11/4	-18/-8	-17.4/-9.0

[†]Using all data at 1,064 nm and infinite wavelength in solution.
[‡]Using data at 1,064 nm only to avoid bias from the dependence of the error on the frequency.
[§]Using data at 1,064 nm and infinite wavelength.

So far we have discussed the main trends of the data in Table 2 and Figure 3 focusing mostly on the performance of the different functionals. However, these data also allows us to draw some important conclusions regarding the adequacy of the PCM-TDDFT combination to account for solvent effects and frequency dependence in hyperpolarizability calculations. In particular, it seems that PCM and TDDFT are insufficient to properly describe these effects. This is best appreciated in Table 3, which shows the differences in averages of errors (ME/MAE) in $\beta_{||}$ at 1,064 nm and infinite wavelength, and in different media for PNA (e.g., in the first row of this Table the average of data at infinite wavelength is subtracted form the average at 1064 nm, which for PBE is 20% in ME and 16% in ME). It is seen by the large differences in errors that all methods have poor solvent dependence of hyperpolarizabilities.

Still, tuned LC-DFT does tend to give smaller differences in errors than the rest of the functionals. The dependence of the error on frequency is in general smaller than for solvent, but not negligible and is quite large (15-20%) for GGAs in particular.

Table 4: Effects of tuning, media, and frequency on the errors in $\beta_{||}$ (with respect to experiment) determined using Yates algorithm on data from Table 2.

(a) Gas and 1,4-Dioxane/Acetone/Methanol		
Variable change	Effect on ME (%)	Effect on MAE (%)
Mean	7.8/-5.5/-11.8	20.8/16.0/20.8
X_1: LC-ωPBE $\longrightarrow$ LC-ωPBE*	19.3/14.5/13.8	6.3/-7.0/-7.8
X_2: Gas $\longrightarrow$ Solution	-1.3/-14.5/-20.75	11.75/7.0/11.8
$X_1 \times X_2$	13.3/8.5/7.8	0.3/-13.0/-13.8
(b) 1,4-Dioxane and Acetone/Acetone and Methanol		
Variable change	Effect on ME (%)	Effect on MAE (%)
Mean	-11.6/-18.4	25.4/22.4
X_1: LC-ωPBE $\longrightarrow$ LC-ωPBE*	20.9/19.4	-7.1/-15.4
X_2: 1,4-Dioxane $\longrightarrow$ Acetone	-0.4	-5.4
X_2: Acetone $\longrightarrow$ Methanol	-6.4	2.4
$X_1 \times X_2$	-0.9/-0.6	-4.9/-3.4
X_3: Inf. $\longrightarrow$ 1,064 nm	4.9/-7.9	2.4/5.4
$X_1 \times X_3$	6.9/2.9	0.4/-5.4
$X_2 \times X_3$	-12.9/0.1	0.6/2.4
$X_1 \times X_2 \times X_3$	-3.9/-0.1	-8.4/2.6

It is also enlightening to carry out an statistical analysis of the effects of tuning, media, and frequency on the error in $\beta_{||}$ utilizing Yates algorithm.[74] This analysis allows to rigorously determine the effect of each of the above variables and their interactions (in the statistical sense) on the error. These results are shown in Table 4 and are interpreted as follows: the mean is the average of the ME/MAE for all calculations considered; a negative value for X_1: LC-ωPBE $\longrightarrow$ LC-ωPBE* refers to a decrease in the mean of the ME/MAE due to tuning and *vice versa*; X_2: Gas $\longrightarrow$ Solution gives the average change in error when going from the gas phase to solution; $X_1 \times X_2$ is the interaction between variables X_1 and X_2, and it is negative if tuning reduces the error when going from gas to solution, etc. So, for example, the MAE of LC-ωPBE in acetone and methanol is 22.4% + 15.4% = 37.8%, whereas for LC-ωPBE* this value is 22.4% - 15.4% = 7%. The data in Table 4 reveal that all variables considered and their interactions can have notable effects on the MEs or MAEs. Large dependence of the errors on the interactions are evidence of the insufficiency

(also discussed above) of the particular PCM-TDDFT combination to describe frequency dependent hyperpolarizabilities in solution. Furthermore, the largely negative values for the effects of X_1: LC-ωPBE $\longrightarrow$ LC-ωPBE* and $X_1 \times X_2$ on the MAEs confirm that tuning tends to improve the description of hyperpolarizabilities, specially in more polar media.

Before closing this discussion regarding PNA, we must note that there are sources of error in our theory-experiment comparisons. Among these, the most notable are the neglect of vibrational contributions to the hyperpolarizability and the error in the experimental $\beta_{||}$ values. However, these errors are likely to be too small to affect the conclusions reached here. For example, the vibrational contributions to $\beta_{||}$ have been estimated to reduce the hyperpolarizability by no more than about 5% at the considered frequencies,[43,75] whereas the error in the gas phase measurement of $\beta_{||}$ is reported to be around 4%.[70] Nonetheless, we provide as a sanity check Table 5. This Table illustrates the improvement of tuned over standard LC-DFT when comparing with static β_{tot} values calculated by the MP2 method, which has been shown to produce reasonably accurate molecular hyperpolarizabilities.[22,40,67,76–78] The qualitative observations that can be drawn from Table 5 are similar to those obtained when using experimental data as reference; LC-DFT tends to underestimate hyperpolarizabilities, the tuning procedure roughly halves this error, and the improvement is more noticeable in polar environments. We also note that, although MP2 tends to somehow overshoot β_{ijk} values compared to coupled cluster calculations, this effect is usually small when using large enough basis sets, similar to the ones used here (see, e.g., Refs. 40 and 43). In addition, LC-ωPBE* and ωB97X-D* have MEs of -4% and -9%, respectively, when compared to MP2. This supports good results from tuned LC-DFT if MP2 is slightly overshooting hyperpolarizabilities. Thus, it seems safe to conclude that tuning the range separation parameter provides a significant improvement on the description of the hyperpolarizability of PNA in different media by LC-DFT.

Table 5: Comparison of MP2 and DFT β_{tot} data (in a.u.) for PNA. All calculations use the 6-311+G(d,p) basis and CAM-B3LYP/6-31G(d,p) geometries.

Media	MP2	LC-ωPBE	LC-ωPBE*	ωB97X-D	ωB97X-D*
Gas	1,616	1,218	1,305	1,337	1,337
1,4-Dioxane	3,019	2,573	3,073	2,507	2,816
Methanol	6,225	4,499	6,634	5,179	6,127
ME (a.u.)	- -	-857	51	-612	-193
MAE (a.u.)	- -	857	258	612	193
ME (%)	- -	-22	-4	-17	-9
MAE (%)	- -	22	9	17	9

DANS in gas phase and solution

We now turn our attention to the performance tuned LC-DFT relative to other DFT methods in the description of the first-order hyperpolarizabilities of the larger DANS molecule. The optimal ω values utilized are listed in Table 6. In Table 7, the predictions of the $\beta_{||}$ values for DANS given by different functionals are compared with static MP2 data in the gas phase, and experimental measurements in $CHCl_3$ at 1,908 nm. There are not nearly as much reference data for DANS as there are for PNA but, nevertheless, the trends regarding LC-DFT errors in this Table mirror those noted for PNA in the preceding discussion. Again, LC-DFT underestimates the first order NLO responses, and the tuning procedure greatly improves results, particularly in solvent media. If anything, we must note that this improvement is much larger for DANS than for PNA; the 62% MAE of LC-ωPBE is reduced to 14% by tuning for DANS, whereas these percentages are 29% and 16% for PNA (Table 2). The absolute errors of tuned LC-DFT are larger for DANS than for PNA, but these errors are similar and remain reasonable percentage wise. This observation is in agreement with the results by Sun and Autschbach.[54]

Table 6: Optimal range separation parameters ($bohr^{-1}$) for DANS.

Media	LC-ωPBE	ωB97X-D
Gas	0.2	0.2
$CHCl_3$	0.1	1×10^{-4}

We also note that, in the gas phase, the optimal LC-ωPBE range separation parameter

Table 7: Comparison of DFT $\beta_{||}$ data (in a.u.) with MP2/6-311++G(d,p) (gas phase, static limit) and experiment (chloroform, 1,908 nm) for DANS. All DFT calculations use the 6-311+G(d,p) basis. The reference MP2 and experimental data have been taken from Ref. 43.

Media	λ	Reference	PBE	LC-ωPBE	LC-ωPBE*	B97-D	ωB97X-D	ωB97X-D*	B3LYP
Gas	Inf.	10,194	23,834	5,960	8,930	23,676	7,680	7,680	16,551
$CHCl_3$	1,908	70,000	153,334	12,692	58,548	152,918	18,614	57,447	66,415
ME (a.u.)	- -	- -	48,487	-30,771	-6,358	48,200	-26,950	-7,534	1,386
MAE (a.u.)	- -	- -	48,487	30,771	6,358	48,200	26,950	7,534	4,971
ME (%)	- -	- -	126	-62	-14	125	-49	-21	29
MAE (%)	- -	- -	126	62	14	125	49	21	34

for DANS (0.2 bohr^{-1}) is smaller than that of PNA (0.3 bohr^{-1}). The inverse relationship between system size and optimal ω has been noticed before[44] and thus, since the default ω in LC-ωPBE is 0.4 bohr^{-1}, it is not surprising that the improvements of tuning are more drastic for DANS compared to PNA. In solution, the minimization of J_{gap} leads to further smaller ω values for DANS, as is the case for PNA too. Furthermore, for both PNA and DANS, the traditional hybrid B3LYP yields rather good results in solution, but largely overestimates gas phase hyperpolarizabilities.

Important differences between the accuracy of DFT predictions for PNA and DANS can also be noticed. The most notable of these is the extremely poor performance of GGAs (over 100% error) for DANS, compared to the relatively good predictions of these functionals for PNA in solution. In this case, the error due to the wrong asymptotic behavior of the DFT exchange potential becomes more severe due to DANS being a larger molecule than PNA. This leads to the well known catastrophic overestimation of the first-order NLO response of GGAs as the system grows larger. Thus, although the optimal ω in LC-DFT decreases with increasing size of the system leading to more "GGA-like" behavior, one should be careful to maintain the correct asymptotic behavior of the exchange. All these observations support the case of tuned LC-DFT being the best choice among DFT methods for predicting hyperpolarizabilities.

Before closing this discussion, a note on the validity of the tuning procedure in larger molecules is germane here. It has been pointed out[79] that tuned LC-DFT is, by construc-

tion, not size-consistent; all of its ingredients are size-consistent, so that tuning breaks this property unless the optimal ω for subsystems A and B, plus noninteracting supersystem $A+B$, are all the same, which is unlikely given the dependence of the optimal ω on system size. By a similar reasoning, tuned LC-DFT is also not expected to be (in general) size-extensive. Thus, one may expect a deterioration of results for tuned LC-DFT as the size of the system increases. This may explain the unsatisfactory results of gap tuning schemes for polarizabilities and second-order hyperpolarizabilities in large π-conjugated chains,[55] as well as the larger absolute errors in $\beta_{||}$ for DANS compared to PNA observed here and in Ref. 54. Nevertheless, it should also be noted that other types of functionals are also known to fail in describing the NLO properties of large molecules, despite being size-extensive (see, e.g., Refs. 54,55). In fact, for first-order hyperpolarizabilities, the increase in error with molecular size of traditional GGAs, hybrids, and LC-DFT is larger than for tuned LC-DFT. Thus, tuning methods still appear to be desirable over standard functionals for the prediction of first-order hyperpolarizabilities.

Diagnostic tool

In the previous examples, we have seen that the accurate prediction of hyperpolarizabilities by DFT depends crucially on the amount of exact exchange incorporated, which can be varied through the tuning of the range-separation parameter in LC-DFT. It is generally recognized, here and elsewhere,[21–25] that pure GGAs tend to overestimate NLO responses, whereas the opposite is true when including large amounts of HF exchange. Tuned LC-DFT can interpolate between these two extremes leading to a more balanced description of hyperpolarizabilities. However, this perspective suggests that, if the usual trends overestimation/underestimation trends of GGAs/HF are not obeyed, then tuned LC-DFT will be unable to improve results significantly over these approaches. This is the basic idea for what could be regarded as a "diagnostic tool" that we propose here to assess whether the prediction of hyperpolarizabilities can be improved by the tuning procedure of LC-DFT.

To illustrate this diagnostic tool consider the pyrrole-based compounds **1** and **2** (see Figure 1 for structures). The hyperpolarizabilities calculated for these compounds using a variety of methods are summarized in Table 8; the errors are also computed using MP2/6-311+G(d,p) data as reference, which are usually very accurate in gas phase[40,43] (see also discussion in the PNA results section). As can be seen from this Table, HF and all DFT methods strongly underestimate the hyperpolarizability ($\sim$ 50% error). It is striking that the strongest underestimations are seen in traditional hybrids (B3LYP) and GGAs (PBE), normally assumed to exaggerate NLO responses. Moreover, the tuning procedure results in a lower $\omega = 0.2$ bohr^{-1} but the hyperpolarizability is reduced (and results worsened) for LC-ωPBE. CAM-B3LYP ($\omega = 0.33$ bohr^{-1}) and ωB97X-D ($\omega = 0.2$ bohr^{-1}) perform similarly to tuned LC-ωPBE. It seems therefore that, since all types of DFT methods largely underestimate β_{tot}, pyrroles **1** and **2** constitute some kind of pathological case for DFT hyperpolarizabilities.

Table 8: Comparison between MP2 and DFT hyperpolarizabilities β_{tot} (in a.u.) for pyrrole-based compound **1** and **2**. All calculations use the 6-311+G(d,p) basis and CAM-B3LYP/6-311++G(d,p) geometries, except CAM-B3LYP, ωB97X-D, and B3LYP which use the 6-311++G(d,p) basis and geometries fully optimized at those levels.

Method	**1**	**2**	ME (%)
MP2	2,387	2,643	- -
HF	1,016	1,215	-56
PBE	510	1,185	-67
LC-ωPBE	1,464	1,790	-35
LC-ωPBE*	1,043	1,535	-49
CAM-B3LYP	1,100	1,578	-47
ωB97X-D	1,132	1,564	-47
B3LYP	670	1,289	-62

To investigate further the cause of this failure of DFT methods in describing the hyperpolarizabilities of **1** and **2**, we analyze the charge transfer properties of these compounds, as well as the relationship between $\beta_{||}$ and ω. Firstly, the difference in density between the ground and excited state are shown in Figure 4. A good degree of charge transfer from the pyrrole to the dicyano and enolate groups for **1** and **2**, respectively, can be appreciated in

this Figure. The indices by Le Bahers et al.[66] D_{CT} and q_{CT}, which measure the distance and charge transferred, respectively, where calculated at the LC-ωPBE/6-311+G(d,p) level to be $D_{CT} = 2.6$ bohr and $q_{CT} = 0.5$ a.u. for **1**, and $D_{CT} = 3.1$ bohr and $q_{CT} = 0.5$ a.u. for **2**. As a reference, for PNA these values are $D_{CT} = 5.2$ bohr and $q_{CT} = 0.6$ a.u. It is notable that, although the hyperpolarizability values of the pyrroles and PNA are similar in magnitude, in **1** and **2** the spatial extent of the charge transfer estimated by D_{CT} is much smaller than for PNA. Nevertheless, **1** and **2** do appear to be charge transfer compounds with NLO properties rather similar to PNA; indeed, assessment of the individual components of β_{tot} reveals that the hyperpolarizability is dominated by a single component in the direction of the dipole moment.

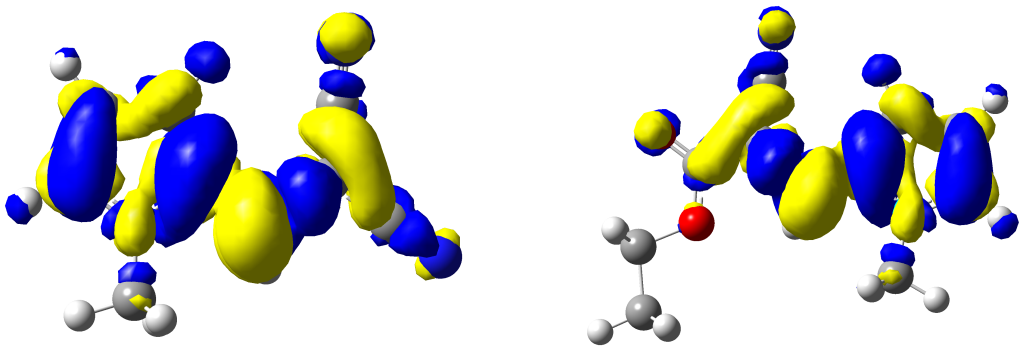

Figure 4: Difference in total electronic density (isocontour value of 0.001 a.u.) between the ground and first two excited states of **1** and **2** at the LC-ωPBE/6-311+G(d,p) level. Yellow (blue) regions indicate a gain (loss) of density in the excited state.

A very striking difference between PNA and the pyrrole compounds is, however, discovered when analyzing the dependence of $\beta_{||}$ as a function of the range separation parameter. Figure 5 shows this difference; it is seen that, for PNA, $\beta_{||}$ decays as ω increases, whereas the opposite is true for **1** and **2** (although there is a small decrease in going from $\omega = 0.4$ bohr^{-1} to $\omega = 0.5$ bohr^{-1}). The behavior of PNA represents some sort of "ideal" for charge-transfer compounds, and it reflects the usual GGA/HF overestimation/underestimation trends as well as other related observations that we have noted in previous studies.[32,52,64,80,81] The opposing trend of the pyrroles could perhaps be related to the much smaller charge transfer

distance D_{CT} in these compounds as compared to PNA. Regardless of that, it is clear that the trends observed for **1** and **2** defy the conventional belief that GGAs overestimate hyperpolarizabilities and that inclusion of HF exchange leads to more moderate NLO responses. Hence, a relationship between the hyperpolarizability and ω similar to that observed for the pyrrole derivatives studied here (i.e., an increase in $\beta_{||}$ along with ω) can serve as diagnostic tool to identify pathological cases in which DFT methods underestimate the NLO response, and the tuning procedure will be unlikely to improve LC-DFT results.

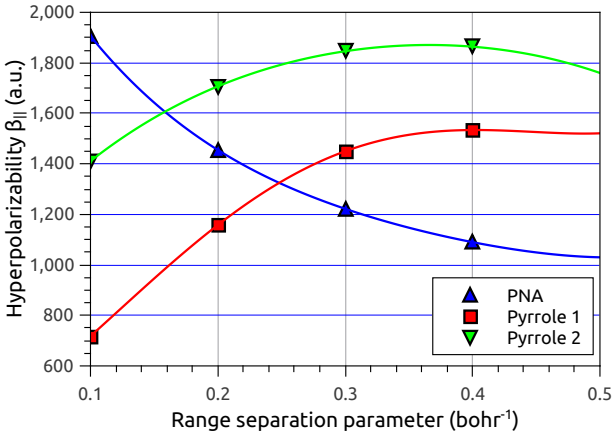

Figure 5: First-order hyperpolarizabilities $\beta_{||}$ at 1,064 nm calculated at the LC-ωPBE/6-311+G(d,p) level as a function of the range separation parameter ω. Tuned LC-DFT will be less likely to improve $\beta_{||}$ in compounds displaying the atypical trend of pyrroles **1** and **2**.

Conclusions

We have shown that a physically motivated, nonempirical, procedure for tuning the range separation parameter in LC-DFT leads to sharp improvements in the description of first-order hyperpolarizabilities in prototypical charge-transfer compounds, such as PNA and DANS, in a wide variety of media. Furthermore, tuned LC-DFT overall performs better than any other type of functionals tested here including standard hybrids, GGAs, and LC-DFT. Nonetheless, we have also identified examples of pathological cases in which all types of DFT methods strongly underestimate the first-order NLO response. However, a simple qualitative tool

based on the dependence between the hyperpolarizability and ω was proposed to identify such cases. We also found that the PCM-TDDFT combination is insufficient to account for the dependence on solvent and frequency of the hyperpolarizabilites, but tuned LC-DFT still can provide a reasonable agreement with experimental results. Caution should also be exercised when calculating properties of large molecules because the tuning procedure is not, in general, size-extensive, so that results deteriorate with increasing system size. Nevertheless, these errors are still smaller for tuned LC-DFT than for traditional GGAs, hybrids, and LC-DFT. Considering all this, we believe that tuned LC-DFT should become a primary choice for the prediction of first-order hyperpolarizabilities among currently available DFT methods.

Acknowledgement

This work was funded by King Abdulaziz University, under grant No. (21-3-1432/HiCi). The authors, therefore, acknowledge technical and financial support of KAU.

References

(1) Maiman, T. H. Stimulated Optical Radiation in Ruby. *Nature* **1960**, 187, 493-494.

(2) Marder, S. R.; Sohn, J. E.; Stucky, G. D. *Materials for Non-linear Optics: Chemical Perspectives*; ACS symposium series 45: Washington, DC, 1991.

(3) Boyd, R. W. *Nonlinear Optics*; Academic Press: New York, 1992.

(4) Marder, S. R. Organic Nonlinear Optical Materials: Where We Have Been and Where We Are Going. *Chem. Commun.* **2006**, 2, 131-134.

(5) Irie, M. Diarylethenes for Memories and Switches. *Chem. Rev.* **2000**, 100, 1685-1716.

(6) Kawata, S; Kawata, Y. Three-Dimensional Optical Data Storage Using Photochromic Materials. *Chem. Rev.* **2000**, 100, 1777-1788.

(7) Tian, H.; Yang, S. Recent Progresses on Diarylethene Based Photochromic Switches. *Chem. Soc. Rev.* **2004**, 33, 85-97.

(8) Dvornikov, A. S.; Walker, E. P.; Rentzepis, P. M. Two-Photon Three-Dimensional Optical Storage Memory. *J. Phys. Chem. A* **2009**, 113, 13633-13644.

(9) Chen, K. J.; Laurent, A. D.; Jacquemin, D. Strategies for Designing Diarylethenes as Ecient Nonlinear Optical Switches. *J. Phys. Chem. C* **2014**, 118, 4334-4345.

(10) Oudar, J. L.; Chemla, D. S. Hyperpolarizabilities of the Nitroanilines and Their Relations to the Excited State Dipole Moment. *J. Chem. Phys.* **1977**, 66, 2664-2668.

(11) Hurst, M.; Munn, R. W. in *Organic Materials for Nonlinear Optics*; Hann, R. A.; Bloor, D., Eds.; The Royal Society of Chemistry: London, 1989.

(12) Kanis, D. R.; Ratner, M. A.; Marks, T. J. Design and Construction of Molecular Assemblies with Large Second-order Optical Nonlinearities. Quantum Chemical Aspect. *Chem. Rev.* **1994**, 94, 195-242.

(13) Ramakrishna, G.; Goodson III, T. Excited-State Deactivation of Branched Two-Photon Absorbing Chromophores: A Femtosecond Transient Absorption Investigation. *J. Phys. Chem. A* **2007**, 111, 993-1000.

(14) Chakrabarti, S.; Ruud, K. Large Two-photon Absorption Cross Section: Molecular Tweezer As a New Promising Class of Compounds for Nonlinear Optics. *Phys. Chem. Chem. Phys.* **2009**, 11, 2592-2596.

(15) Kurtz, H.; Dudis, D. Quantum Mechanical Methods for Predicting Nonlinear Optical Properties. *Rev. Comput. Chem.* **1998**, 12, 241-279.

(16) Shelton, D. P.; Rice, J. E. Measurements and Calculations of the Hyperpolarizabilities of Atoms and Small Molecules in the Gas Phase. *Chem. Rev.* **1994**, 94, 3-29.

(17) Sim, F.; Chin, S.; Dupuis, M.; Rice, J. E. Electron Correlation Effects in Hyperpolarizabilities of p-Nitroaniline. *J. Phys. Chem.* **1993**, 97, 1158-1163.

(18) Tawada, Y.; Tsuneda, T.; Yanagisawa, S.; Yanai, T.; Hirao, K. A Long-range-corrected Time-dependent Density Functional Theory. *J. Chem. Phys.* **2004**, 120, 8425-8433.

(19) Bulat, F. A.; Toro-Labbé, A; Champagne, B.; Kirtman, B.; Yang, W. Density-functional Theory (Hyper)polarizabilities of Push-pull π-Conjugated Systems: Treatment of Exact Exchange and Role of Correlation. *J. Chem. Phys.*, **2005**, 123, 014319(1-7).

(20) Bokhan, D.; Bartlett, R. J. Exact-exchange Density Functional Theory for Hyperpolarizabilities. *J. Chem. Phys.* **2007**, 127, 174102(1-9).

(21) Champagne, B.; Perpète, E. A.; van Gisbergen, S. J. A.; Baerends, E. J.; Snijders, J. G.; Soubra-Ghaoui, C. ; Robins, K. A.; Kirtman, B. Assessment of Conventional Density Functional Schemes for Computing the Polarizabilities and Hyperpolarizabilities of Conjugated Oligomers: An ab Initio Investigation of Polyacetylene Chains. *J. Chem. Phys.* **1998**, 109, 10489-10498.

(22) Champagne, B.; Perpète, E. A.; Jacquemin, D.; van Gisbergen, S. J. A.; Baerends, E. J.; Soubra-Ghaoui, C.; Robins, K. A.; Kirtman, B. Assessment of Conventional Density Functional Schemes for Computing the Dipole Moment and (Hyper)polarizabilities of Push-Pull π-Conjugated Systems. *J. Phys. Chem. A* **2000**, 104, 4755-4763.

(23) Loboda, O.; Zaleśny, R.; Avramopoulos, A.; Luis, J. M.; Kirtman, B.; Tagmatarchis, N.; Reis, H.; Papadopoulos, M. G. Linear and Nonlinear Optical Properties of [60]Fullerene Derivatives. *J. Phys. Chem. A* **2009**, 113, 1159-1170.

(24) van Faassen, M.; de Boeij, R.; van Leeuwen, P. L.; Berger, J. A.; Snijders, J. G. Application of Time-dependent Current-density-functional Theory to Nonlocal Exchange-correlation Effects in Polymers. *J. Chem. Phys.* **2003**, 118, 1044-1053.

(25) Kirtman, B.; Lacivita, V.; Dovesi, R.; Reis, H. Electric Field Polarization in Conventional Density Functional Theory: From Quasilinear to Two-dimensional and Three-dimensional Extended Systems. *J. Chem. Phys.* **2011**, 135, 154101(1-10).

(26) Savin, A.; Flad, H. Density Functionals for the Yukawa Electron-electron Interaction. *Int. J. Quantum Chem.* **1995**, 56, 327-332.

(27) Iikura, H.; Tsuneda, T.; Yanai, T.; Hirao, K. A Long-range Correction Scheme for Generalized-gradient-approximation Exchange Functionals. *J. Chem. Phys.* **2001**, 115, 3540-3544.

(28) Yanai, T.; Tew, D. P.; Handy, N. C. A New Hybrid Exchange-correlation Functional Using the Coulomb-attenuating Method (CAM-B3LYP). *Chem. Phys. Lett.* **2004**, 393, 51-57.

(29) Vydrov, O. A.; Heyd, J.; Krukau, A. V.; Scuseria, G. E. Importance of Short-range Versus Long-range Hartree-Fock Exchange for the Performance of Hybrid Density Functionals. *J. Chem. Phys.* **2006**, 125, 074106(1-9).

(30) Vydrov, O. A.; Scuseria, G. E. Assessment of a Long-range Corrected Hybrid Functional. *J. Chem. Phys.* **2006**, 125, 234109(1-9).

(31) Jacquemin, D.; Perpète, E. A.; Vydrov, O. A.; Scuseria, G. E.; Adamo, C. Assessment of Long-range Corrected Functionals Performance for $n \longrightarrow \pi^*$ Transitions in Organic Dyes. *J. Chem. Phys.* **2007**, 127, 094102(1-6).

(32) Garza, A. J.; Scuseria, G. E.; Khan, S. B.; Asiri, A. M. Assessment of Long-range Corrected Functionals for the Prediction of Non-linear Optical Properties of Organic Materials *Chem. Phys. Lett.* **2013**, 575, 122-125.

(33) Lu, S.-I. Assessment of the Global and Range-separated Hybrids for Computing the

Dynamic Second-order Hyperpolarizability of Solution-phase Organic Molecules. *Theor. Chem. Acc.* **2014**, 133, 1439.

(34) Kamiya, M.; Sekino, H.; Tsuneda, T.; Hirao, K. Nonlinear Optical Property Calculations by the Long-range-corrected Coupled-perturbed Kohn-Sham Method. *J. Chem. Phys.* **2005**, 122, 234111(1-10).

(35) Jacquemin, D.; Perpète, E. A.; Scuseria, G. E.; Ciofini, I.; Adamo, C. TD-DFT Performance for the Visible Absorption Spectra of Organic Dyes: Conventional versus Long-Range Hybrids. *J. Chem. Theory Comput.* **2008**, 4, 123-135.

(36) Perpète, E. A.; Jacquemin, D.; Adamo, C.; Scuseria, G. E. Revisiting the Nonlinear Optical Properties of Polybutatriene and Polydiacetylene with Density Functional Theory. *Chem. Phys. Lett.* **2008**, 456, 101-104.

(37) Jacquemin, D.; Perpète, E. A.; Scuseria, G. E.; Ciofini, I. Adamo, C. Extensive TD-DFT Investigation of the First Electronic Transition in Substituted Azobenzenes. *Chem. Phys. Lett.* **2008**, 465, 226-229.

(38) Song, J.; Watson, M. A.; Sekino, H.; Hirao, K. Nonlinear Optical Property Calculations of Polyynes with Long-range Corrected Hybrid Exchange-correlation Functionals. *J. Chem. Phys.* **2008**, 129, 024117(1-8).

(39) Zaleśny, R.; Bulik, I. W.; Bartkowiak, W.; Luis, J. M.; Avramopoulos, A.; Papadopoulos, M. G.; Krawczyk, P. Electronic and Vibrational Contributions to First Hyperpolarizability of Donor-acceptor-substituted Azobenzene. *J. Chem. Phys.* **2010**, 133, 244308(1-7).

(40) de Wergifosse M.; Champagne, B. Electron Correlation Effects on the First Hyperpolarizability of Push-pull π-Conjugated Systems. *J. Chem. Phys.* **2011**, 134, 074113(1-13).

(41) Jacquemin, D.; Perpète, E. A.; Medved, M.; Scalmani, G.; Frisch, M. J.; Kobayashi, R.; Adamo, C. First Hyperpolarizability of Polymethineimine with Long-range Corrected Functionals. *J. Chem. Phys.* **2007**, 126, 191108(1-4).

(42) Nguyen, K. A.; Rogers, J. E.; Slagle, J. E.; Day, P. N.; Kannan, R.; Tan, L.; Fleitz, P. A.; Pachter, R. Effects of Conjugation in Length and Dimension on Spectroscopic Properties of Fluorene-Based Chromophores from Experiment and Theory. *J. Phys. Chem. A* **2006**, 110, 13172-13182.

(43) Day, P. N.; Pachter, R.; Nguyen, K. A. Analysis of Nonlinear Optical Properties in Donor-acceptor Materials. *J. Chem. Phys.* **2014**, 140, 184308(1-13).

(44) Refaely-Abramson, S.; Baer, R.; Kronik, L. Fundamental and Excitation Gaps in Molecules of Relevance for Organic Photovoltaics From an Optimally Tuned Range-separated Hybrid Functional. *Phys. Rev. B* **2011**, 84, 075144(1-8).

(45) Stein, T.; Kronik, L.; Baer, R. Reliable Prediction of Charge Transfer Excitations in Molecular Complexes Using Time-Dependent Density Functional Theory. *J. Am. Chem. Soc.* **2009**, 131, 2818-2820.

(46) Stein, T.; Kronik, L.; Baer, R. Prediction of Charge-transfer Excitations in Coumarin-based Dyes Using a Range-separated Functional Tuned From First Principles. *J. Chem. Phys.* **2009**, 131, 244119(1-5).

(47) Stein, T.; Eisenberg, H; Kronik, L.; Baer, R. Fundamental Gaps in Finite Systems from Eigenvalues of a Generalized Kohn-Sham Method. *Phys. Rev. Lett.* **2010**, 105, 266802(1-4).

(48) Karolewski, A.; Stein, T.; Kümmel, S. Tailoring the Optical Gap in Light-harvesting Molecules. *J. Chem. Phys.* **2011**, 134, 151101(1-4).

(49) Autschbach, J.; Srebro, M. Delocalization Error and Functional Tuning in Kohn-Sham Calculations of Molecular Properties. *Acc. Chem. Res.* DOI: 10.1021/ar500171t.

(50) Koopmans, T. Über die Zuordnung von Wellenfunktionen und Eigenwerten zu den einzelnen Elektronen eines Atoms. *Physica* **1934**, 1, 104-113.

(51) Pandey, L.; Doiron, C.; Sears, J. S.; Brédas, J. Lowest Excited States and Optical Absorption Spectra of Donor-Acceptor Copolymers for Organic Photovoltaics: A New Picture Emerging From Tuned Long-range Corrected Density Functionals. *Phys. Chem. Chem. Phys.* **2012**, 14, 14243-14248.

(52) Garza, A. J.; Osman, O. I.; Wazzan, N. A.; Khan, S. B.; Asiri, A. M.; Scuseria, G. E. A Computational Study of the Nonlinear Optical Properties of Carbazole Derivatives: Theory Refines Experiment. *Theor. Chem. Acc.* **2014**, 133, 1458.

(53) Zhang, C.; Sears, J. S.; Yang, B.; Aziz, S.; Coropceanu, V; Brédas, J. Theoretical Study of the Local and Charge-Transfer Excitations in Model Complexes of Pentacene-C_{60} Using Tuned Range-Separated Hybrid Functionals. *J. Chem. Theory Comput.* **2014**, 10, 2379-2388.

(54) Sun, H.; Autschbach, J. Influence of the Delocalization Error and Applicability of Optimal Functional Tuning in Density Functional Calculations of Nonlinear Optical Properties of Organic Donor-Acceptor Chromophores. *ChemPhysChem* **2013**, 14, 2450-2461.

(55) Nénon, S.; Champagne, B.; Spassova, M. I. Assessing Long-range Corrected Functionals With Physically-adjusted Range-separated Parameters for Calculating the Polarizability and the Second Hyperpolarizability of Polydiacetylene and Polybutatriene Chains. *Phys. Chem. Chem. Phys.* **2014**, 17, 7083-7088.

(56) Asiri, A. M.; Faidallah, H. M.; Al-Thabaiti, S. A.; Ng, S. W.; Tiekink, E. R. T. 2-[(1-Methyl-1H-pyrrol-2-yl)methylidene]propanedinitrile. *Acta Cryst.* **2012**, E68, o1170.

(57) Asiri, A. M.; Al-Youbi, A. O.; Alamry, K. A.; Faidallah, H. M.; Ng, S. W.; Tiekink, E. R. T. Ethyl (2E)-2-cyano-3-(1-methyl-1H-pyrrol-2-yl)prop-2-enoate. *Acta Cryst.* **2011**, E67, o2315.

(58) Willets, A.; Rice, J. E.; Burland, D. M.; Shelton, D. Problems in the Comparison of Theoretical and Experimental Hyperpolarizabilities. *J. Chem. Phys.* **1992**, 97, 7590-7599.

(59) Stäehlin, M.; Moylan, C. R.; Burland, D. M.; Willets, A.; Rice, J. E.; Shelton, D. P.; Donley, E. A. A Comparison of Calculated and Experimental Hyperpolarizabilities for Acetonitrile in Gas and Liquid Phases. *J. Chem. Phys.* **1993**, 98, 5595-5603.

(60) Reis, H. Problems in the Comparison of Theoretical and Experimental Hyperpolarizabilities Revisited. *J. Chem. Phys.* **2006**, 125, 014506(1-9).

(61) Perdew, J. P.; Parr, R. G.; Levy, M.; Balduz, J. L. Density-Functional Theory for Fractional Particle Number: Derivative Discontinuities of the Energy. *Phys. Rev. Lett.* **1982**, 49, 1691-1694.

(62) Almbladh, C.-O.; von-Barth, U. Exact Results for the Charge and Spin Densities, Exchange-correlation Potentials, and Density-functional Eigenvalues *Phys. Rev. B: Condes. Matter* **1985**, 31, 3231-3244.

(63) Champagne, B.; Kirtman, B. Evaluation of Alternative Sum-over-states Expressions for the First Hyperpolarizability of Push-pull π-Conjugated Systems. *J. Chem. Phys.* **2006**, 125, 024101(1-7).

(64) Garza, A. J.; Osman, O. I.; Wazzan, N. A.; Khan, S. B.; Asiri, A. M.; Scuseria, G. E. Prediction of the Linear and Nonlinear Optical Properties of Tetrahydronaphthalone Derivatives Via Long-range Corrected Hybrid Functionals. *Mol. Phys.* **2014**, DOI: 10.1080/00268976.2014.934312.

(65) Gaussian 09, Revision A.02, Frisch MJ, Trucks GW, Schlegel HB et al., Gaussian Inc., Wallingford, CT, 2009.

(66) Le Bahers, T.; Adamo, C.; Ciofini, I. A Qualitative Index of Spatial Extent in Charge-Transfer Excitations. *J. Chem. Theory Comput.* **2011**, 7, 2498-2506.

(67) Suponitsky, K. Y.; Tafur, S.; Masunov, A. E. Applicability of Hybrid Density Functional Theory Methods to Calculation of Molecular Hyperpolarizability. *J. Chem. Phys.* **2008**, 129, 044109(1-11).

(68) GaussView, Version 5, Dennington R, Keith T, Millam J, Semichem Inc., Shawnee Mission KS, 2009.

(69) Tomasi, J.; Mennucci, B.; Cammi, R. Quantum Mechanical Continuum Solvation Models. *Chem. Rev.* **2005**, 105, 2999-3094.

(70) Kaatz, P.; Donley, E. A.; Shelton, D. P. A Comparison of Molecular Hyperpolarizabilities From Gas and Liquid Phase Measurements. *J. Chem. Phys.* **1997**, 108, 849-856.

(71) Teng, C. C.; Garito, A. F. Dispersion of the Nonlinear Second-order Optical Susceptibility of Organic Systems. *Phys. Rev. B* **1983**, 28, 6766-6773.

(72) Cheng, L.-T.; Tam, W.; Stevenson, S. H.; Meredith, G. R.; Rikken, G.; Marder, S. R. Experimental Investigations of Organic Molecular Nonlinear Optical Polarizabilities. 1. Methods and Results on Benzene and Stilbene Derivatives. *J. Phys. Chem.* **1991**, 95, 10631-10643.

(73) Cheng, L.-T.; Tam, W.; Stevenson, S. H.; Meredith, G. R.; Rikken, G.; Marder, S. R. Experimental Investigations of Organic Molecular Nonlinear Optical Polarizabilities. 2. A Study of Conjugation Dependences. *J. Phys. Chem.* **1991**, 95, 10643-1052.

(74) Box, G. E. P.; Hunter, W. G.; Hunter, J. S. *Statistics for Experimenters: An Introduction to Design, Data Analysis, and Model Building*; John Wiley and Sons: New York, 1978; pp 306-345.

(75) Quinet, O.; Champagne, B.; Kirtman, B. Zero-point Vibrational Averaging Correction for Second Harmonic Generation in Para-nitroaniline. *J. Mol. Struct.: THEOCHEM* **2003**, 633, 199-207.

(76) Hammond, B. L.; Rice, J. E. *Ab Initio* Determination of the Nonlinear Optical properties of HCl. *J. Chem. Phys.* **1992**, 97, 1138-1143.

(77) Lu, S.-I. Computational Study of Static First Hyperpolarizability of Donor-acceptor Substituted (E)-Benzaldehyde Phenylhydrazone. *J. Comput. Chem.* **2011**, 32, 730-736.

(78) de Wergifosse M.; Wautelet, F.; Champagne, B.; Kishi, R.; Fukuda, K.; Matsui, H.; Nakano, M. Challenging Compounds for Calculating Hyperpolarizabilities: p-Quinodimethane Derivatives. *J. Phys. Chem. A* **2013**, 117, 4709-4715.

(79) Karolewski, A.; Kronik, L.; Kümmel, S. Using Optimally Tuned Range Separated Hybrid Functionals in Ground-state Calculations: Consequences and Caveats. *J. Chem. Phys.* **2013**, 138, 204115(1-11).

(80) Garza, A. J.; Osman, O. I.; Scuseria, G. E.; Wazzan, N. A.; Khan, S. B.; Asiri, A. M. Nonlinear Optical Properties of DPO and DMPO: A Theoretical and Computational Study. *Theor. Chem. Acc.* **2013**, 132, 1384.

(81) Garza, A. J.; Osman, O. I.; Wazzan, N. A.; Khan, S. B.; Scuseria, G. E.; Asiri, A. M. Photochromic and Nonlinear Optical Properties of Fulgides: A density Functional Theory Study. *Comput. Theor. Chem.* **2013**, 1022, 82-85.

Graphical TOC Entry